

# EUROPEAN ORGANIZATION FOR NUCLEAR RESEARCH

## Proposal to the ISOLDE and Neutron Time-of-Flight Committee

### Study of molybdenum oxide by means of Perturbed Angular Correlations and Mössbauer spectroscopy

[11.Jan.2016]

Juliana Schell<sup>1,2</sup>, João Guilherme Martins Correia<sup>1,3</sup>, Katharina Lorenz<sup>4</sup>, Marco Peres<sup>4</sup>, Carlos Díaz-Guerra<sup>5</sup>, H.P. Gunnlaugsson<sup>1,6</sup>, Aitana Tarazaga<sup>7</sup>, Manfred Deicher<sup>2</sup>

<sup>1</sup> ISOLDE-CERN, Switzerland

<sup>2</sup> Universität des Saarlandes, Germany

<sup>3</sup> Centro de Ciências e Tecnologias Nucleares (C<sup>2</sup>TN), Instituto Superior Técnico, Universidade de Lisboa, Portugal

<sup>4</sup> Instituto de Plasmas e Fusão Nuclear, Instituto Superior Técnico, Universidade de Lisboa, Portugal

<sup>5</sup> Dpto. Física de Materiales, Facultad de Ciencias Físicas, Universidad Complutense de Madrid, Spain

<sup>6</sup> KU Leuven, Instituut voor Kern- en Stralingsfysica, 3001 Leuven, Belgium

<sup>7</sup> Johannes Kepler University, Linz, Austria

Spokesperson(s): João Guilherme Martins Correia [joao@cern.ch](mailto:joao@cern.ch)

Local contact: Juliana Schell [juliana.schell@cern.ch](mailto:juliana.schell@cern.ch)

#### Abstract

Among transition-metal oxides, the Molybdenum oxide compounds are particularly attractive due to the structural (2D) anisotropy and to the ability of the molybdenum ion to change its oxidation state, being such properties well adequate for applications on, e.g., chemical sensors, solar cells, catalytic and optoelectronic devices. At ISOLDE we aim studying the incorporation of selected dopants by ion implantation, using the nuclear techniques of Perturbed Angular Correlations (PAC) and Mössbauer spectroscopy (MS). Both techniques make use of highly diluted radioactive probe nuclei, which interact – as atomic sized tips – with the host atoms and defects. The objectives of this project are to study at the atomic scale the probe's local environment, its electronic configuration and polarization, the probe's lattice sites, point defects and its recombination dynamics and, in the case of e-gamma PAC, the electron mobility on the host can be further studied, e.g., as a function of temperature.

**Requested shifts:** 9 shifts, (split over 2 years subject to the ISOLDE schedule)



## About Molybdenum oxide

MoO<sub>3</sub> belongs to the family of 2D inorganic materials that are attracting increasing attention because of their distinct properties and high specific surface areas [MAS2011]. The room temperature stable orthorhombic  $\alpha$ -MoO<sub>3</sub> phase is a wide band gap semiconductor (2.8 – 3.2 eV) of most practical interest because of its anisotropic layered structure parallel to (010) planes. Due to such structural characteristics,  $\alpha$ -MoO<sub>3</sub> has been demonstrated to have promising performance in solar cells [GIR2011], catalysis [LAB2001], gas sensing [COM2005], field emission [ZHO2003], lithium-ion batteries [HU2015], photochromic and electrochromic devices [YAO1992].

Oxygen vacancies play a key role in the physical properties of Mo-oxides, since they introduce gap states and influence their optical band gap as well as their electrical conductivity. The oxygen defect concentration is determined by the oxygen partial pressure and preparation temperatures, which also influence crystal morphology. Thermal treatments under low oxygen partial pressures, mechanical activation or UV-irradiation of MoO<sub>3</sub> induce oxygen defects and lead to MoO<sub>3-x</sub> [PEN2014]. The proper combination of several Mo oxides or an adequate distribution of Mo ions with different oxidation states may lead to materials with new electronic and optical properties. For instance, MoO<sub>3</sub> is a transparent semiconductor, while MoO<sub>2</sub> is a metallic conductor. To gain a deeper insight into these phenomena, it is of great importance to systematically investigate the relationship between geometric and electronic structures in MoO<sub>3</sub>.

The hole mobility of intrinsic  $\alpha$ -MoO<sub>3</sub> was reported to be relatively high. However, the resistivity of intrinsic  $\alpha$ -MoO<sub>3</sub> is very high. To overcome this issue, doping with several cations, e.g. In, has been proposed [HAN2011]. In a different application, Cd-doped  $\alpha$ -MoO<sub>3</sub> nanobelts revealed that the synthesized samples not only exhibit high response to H<sub>2</sub>S but also small cross-sensing to other reducing gases. The change of intrinsic defects in the Cd-doped samples is responsible for the enhancement of the sensing properties as shown by PL, Raman and XPS measurements [BAI2014]. On the other hand, in spite of their interesting properties, MoO<sub>3</sub> samples normally show low luminescence emission efficiency [SON2012]. Strong and stable room-temperature photoluminescence has recently been achieved in MoO<sub>3</sub> crystals doped with Er and Eu by ion implantation [VIL2014]. Rare earth (RE) doping is also beneficial for applications in organic solar cells [WAN2012].

The physics behind these multiple applications is linked with the nanoscopic phenomenology, such as oxygen vacancies, point defects and impurity doping. Based on these issues we aim using the Perturbed Angular Correlation (PAC) and emission Mössbauer Spectroscopy (eMS) nuclear radioactive techniques to study high crystalline quality molybdenum trioxide lamellar crystals. These techniques provide information at the atomic scale due to the sensing of the local electronic charge densities (Electric Field Gradient – EFG) for the case of PAC and the polarization (Hyperfine Magnetic field – B) on the probe's environment by eMS. The interpretation of the experimental data will be complemented using Density Functional Theory (DFT) calculations.

## Description of the Proposed Work

- $\alpha$ -MoO<sub>3</sub> lamella crystals will be grown by a sublimation method. Growth conditions were optimised previously [VIL2014]. Pure Mo powder is compacted under compressive load to form disks which are introduced in a quartz tube and annealed at 750 °C for 10 h in a horizontal tube furnace in air. Using these conditions, a large amount of high quality  $\alpha$ -MoO<sub>3</sub> lamella crystals is deposited on the cooler part of the internal wall of the tube.
- Selected radioactive probe elements for PAC will be implanted at ISOLDE: <sup>111</sup>In(<sup>111</sup>Cd), <sup>111m</sup>Cd(<sup>111</sup>Cd), <sup>117</sup>Cd(<sup>117</sup>In), <sup>115</sup>Cd(<sup>115</sup>In).
- After implantation the samples are first studied as a function of annealing temperature and annealing atmosphere to reduce/remove implantation damage. Annealing can also be used to tune the concentration of oxygen vacancies to be later studied. Additionally, the stability of the dopant on the lattice can be studied as a function of annealing time and temperature. After annealing the PAC measurements can be performed as a function of temperature covering the interesting temperature range providing information about the dopant – host interactions which are temperature dependent.
- One particular case study combines <sup>111m</sup>Cd e- $\gamma$  PAC with  $\gamma$ - $\gamma$  PAC on the same isotope – same sample. e- $\gamma$  PAC starts the measurement after ejection of a K shell conversion electron. The recombination time of the deep electronic shells is very fast much below PAC ns time resolution. However the ionisation of the uppermost shells, can exist for time enough to be observable from ns – to micros. This recombination time is essentially a function of the electron carrier concentration and mobility of the host. Then the observable PAC spectra describe transient changes which can be used to learn about existing excited electronic states at the probe atom, and their half-lives as a function of the host electron mobility [LUP1996, COR2016].
- Therefore, using a combination of PAC experiments measuring the hyperfine fields at In and Cd probes, we can study the incorporation of these relevant dopants of MoO<sub>3</sub> at an atomic scale, follow defects recovery, oxygen vacancies and their interaction with the dopants, look for the temperature dependence of atomistic and electronic phenomena and, finally, look for long-lived (t > ns) excited states at the atomic probe Cd and study the electron mobility of the different samples via the use of e-g PAC.
- Selected Radioactive probe elements for eMS will be implanted: <sup>57</sup>Mn(<sup>57</sup>Fe), <sup>119</sup>In(<sup>119</sup>Sn), <sup>151</sup>Gd(<sup>151</sup>Eu), <sup>166</sup>Ho(<sup>166</sup>Er)
- Using the Mössbauer technique we aim at performing a similar program of studies to the PAC on complementary Fe and Sn probes and the particularly relevant optically active Er and Eu elements to investigate the annealing of implantation defects, the probe's lattice location and the probes-host or probes-defects interactions as a function of sample stoichiometry, annealing and measurements temperature. In the case of very short lived probes the annealing and measuring temperatures are the same.
- Complementary characterisation will be performed at the participants home institutions, including energy dispersive X-ray microanalysis, micro-

photoluminescence and micro-Raman spectroscopies, X-ray diffraction, Ion Beam Analysis and electrical characterisation using I-V curves. Preliminary I-V curves show a strong increase of conductivity directly after annealing in vacuum. However, this effect is only temporary lasting for several hours. One aim of this project is to find processes to reproducibly control and engineer the material's properties.

### **About the PAC Spectroscopy technique**

Perturbed Angular Correlations, PAC, appears in this context as an exotic nuclear technique, where each radioactive atom embedded in the sample acts as local spy of its own environment. Actually, the nuclear quadrupole moment, (due to the non-spherical symmetry of the excited nuclear state) and its magnetic moment interact with their immediate environment. By "environment" we refer to the electronic charge density, symmetry, distribution, and polarization, resulting from the crystalline structure, the atomic shells and chemical bonding originating the crystal field or additionally revealing point defects in the probe nuclei neighbourhood. This is done via the so-called nucleus – electrons "hyperfine interaction", which establishes an additional energy splitting at the probing nuclear intermediate excited state, of the order of  $10^{-7}$  eV. The PAC method requires an excited cascade decaying via two gammas or a conversion electron and a gamma where the nuclear quadrupole and magnetic moments of the intermediate state are the probing nuclear features. The advantages regarding traditional Nuclear Magnetic / Quadrupole Resonance techniques are, on the one hand, the fact that a panoply of radioactive elements exist with excited states of suitable nuclear spin and nuclear moments, differently from stable nuclei with a reduced number of probing cases. On the other hand, the amount of radioactive nuclei, which are necessary to perform experiments, is generally less than  $10^{12}$  radioactive atoms, at highly diluted concentrations generally, in the range between 0.01% and ppm, while for normal hyperfine techniques concentrations at the % range are required. This amount of atoms is still enough to produce an observable modulation of the decay curve, described by the so called anisotropy ratio,  $R(t)$ . A fit to this curve allows identifying multiple fractions of probe atoms interacting with certain local environments. Compared with Mössbauer spectroscopy PAC measures, as well, hyperfine quadrupole / EFG and magnetic hyperfine fields, but it is not sensitive to the absolute variation of the energy of the probing state, i.e., the - chemical shift – that provides already information regarding the chemical bonding. Differently from MS, PAC has the advantage that the signal sensitivity is unchanged at any temperature above 0.1K. An additional feature is that the measurement of the PAC signal consists of a time differential analysis of the variation of the consecutive probability that the first gamma (electron) is emitted followed by the second gamma on the decay cascade on a precise direction of space. The observable variations translate the energy splitting as frequencies that fully characterize the charge symmetry and density (Electric Field Gradient, EFG) and magnetic hyperfine fields aimed to probe. Transient phenomena occurring at the time scale of the measurements, from ns to  $\mu$ s can also be observed. Further, in the case of the electron – gamma technique where additional information can be obtained upon electronic recombination at the atomic shells and the neighbour atoms after the emission of the conversion electron from the probe nuclei K, L, or M atomic shells. Phenomena such as the observation of lattice sites, defects, polaron excitations, orbital ordering, electronic polarization, the whole being observed as a function of a multitude of parameters like temperature, electric field, and pressure are examples of the potentiality of the PAC technique that we want now apply to the present set of materials and problematic

under study. A more detailed description of the PAC technique can be found in references [ABRA1953] [SCH1996].

**Resume of our earlier findings:**

Preliminary PAC experiments were done on  $\alpha$ -MoO<sub>3</sub> lamella crystals at ISOLDE-CERN to study the recovery of defects and the local environment of implanted <sup>111m</sup>Cd as a function of annealing and measuring temperatures. Samples were subject to annealing treatments in air up to 723K, temperature that was found to be optimal for recovering of implantation defects as seen by the PAC measurements. PAC spectra for different measurement temperatures are shown in the figure 1.

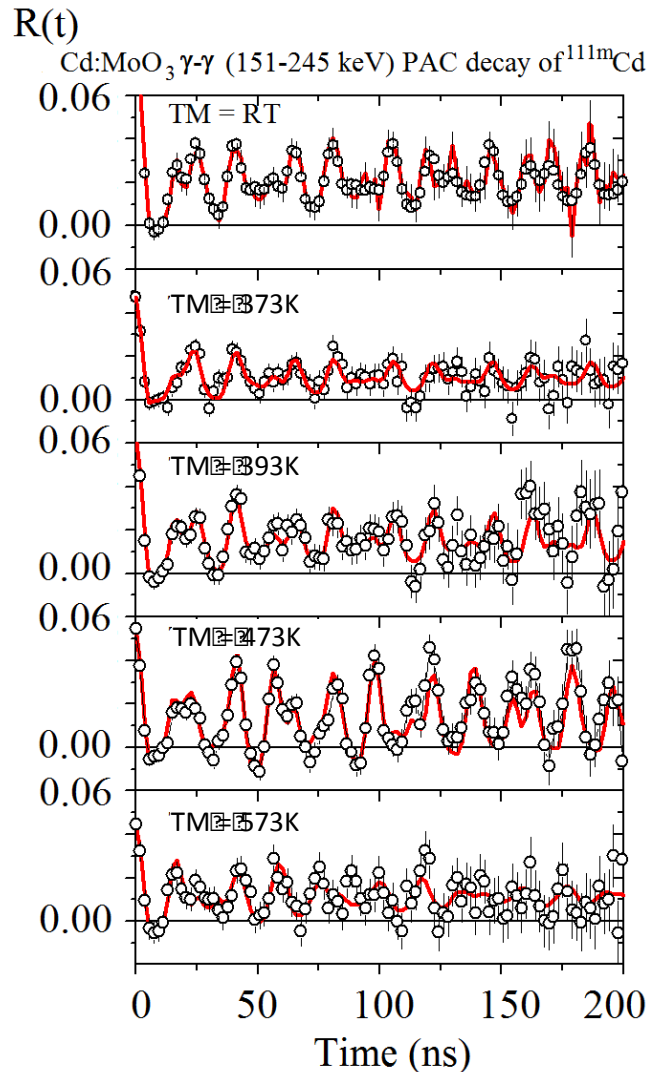
The electric field gradients (EFG) measured for <sup>111m</sup>Cd/Cd show evidence for Cd interacting with two regular environments on MoO<sub>3</sub>, one being substitutional at Mo and the other due to the interaction with a point defect, maybe an oxygen vacancy – both interpretations subject to further studies and the confirmation by DFT simulations. The fraction of probes occupying each site respectively increase/decrease with temperature showing a reversible and interrelated behaviour that hints at the observation of a dynamic atomic rearrangement of the dopant Cd with the defect as a function of temperature. Thorough studies shall confirm the reproducibility of the measurements and allow determining the atomistic configurations of the probe – lattice and probe – defect – lattice and extract activation energies.

**About the Mössbauer Spectroscopy technique**

Mössbauer spectroscopy gives a wealth of information of the probe atoms, such as charge state, site symmetry, magnetic properties and binding properties. Usually 3-5 different probe environments can be distinguished. With emission Mössbauer spectroscopy, one can measure highly diluted samples (<10<sup>-3</sup> at.%) where the probes can be used to measure the properties of the material on the atomic scale.

**Resume of our earlier findings:**

Figure 1: PAC spectra, R(t) observable anisotropy ratio function as a function of time of molybdenum oxide annealed at 723K at different measurement temperature using <sup>111m</sup>Cd/Cd as probe nuclei.



In test experiments that were a part of the IS501 experiment, we implanted  $^{119}\text{In}$  and  $^{57}\text{Mn}$  into amorphous  $\text{MoO}_x$  samples (nominally  $x=3$ ).

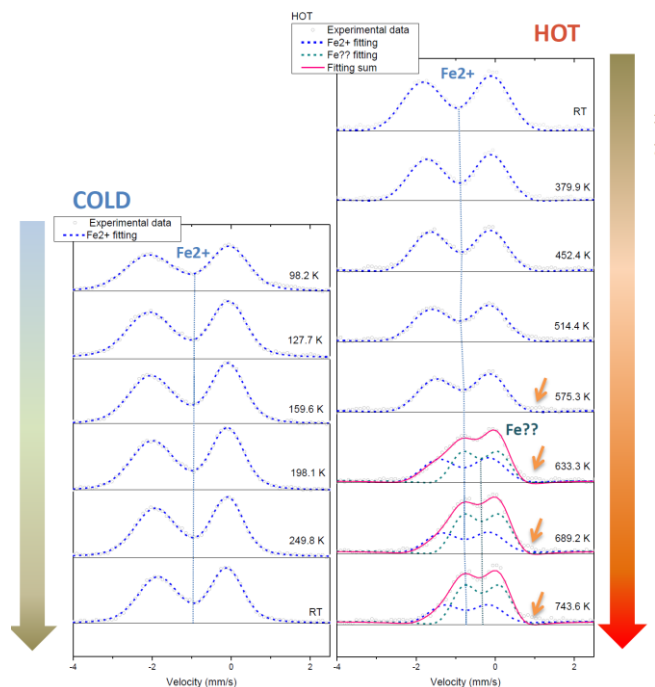


Figure 2:  $^{57}\text{Fe}$  eMS spectra obtained after implantation of  $^{57}\text{Mn}$  into amorphous  $\text{MoO}_x$  samples held at the temperature indicated.

Three different behaviours could be detected: At  $T < -123$  °C, the probe atoms come to rest in highly defective areas and are characterized as high spin  $\text{Fe}^{2+}$  with very low binding to the lattice. At  $-123^\circ\text{C} < T < 327$  °C, the probe atoms are characterized as high spin  $\text{Fe}^{2+}$  in amorphous state. At  $T > 327^\circ\text{C}$ , the shift of lines and decreased splitting evidences that the sites get more covalent character and exhibit stronger binding to the lattice; this happens when the  $\text{MoO}_x$  recrystallizes. Similar results were obtained using  $^{119}\text{In}$  (not shown here).

These results demonstrate that  $\text{MoO}_x$  is well suited for implantation (defects anneal at relatively low temperatures), but much further work is needed to understand the nature of the sites.

One of the outstanding dilemma is why Fe is observed only as  $\text{Fe}^{2+}$ , and not as  $\text{Fe}^{3+}$ ? One possibility is that the sites are associated with donor type defects that do not anneal at  $477^\circ\text{C}$ . In this case, angular dependent measurements on crystalline samples and measurements at higher temperatures can elucidate these questions. Implantations with longer lived probes, such as  $^{119}\text{Sb}$  ( $T_{1/2} = 38$  h) or  $^{57}\text{Co}$  ( $T_{1/2} = 272$  d) can also be used in this context, where there are better possibilities for annealing studies in particular with view to the reversible changes observed in our preliminary electrical measurements after annealing.

The results shown in Figure 2:  $^{57}\text{Fe}$  eMS spectra obtained after implantation of  $^{57}\text{Mn}$  into amorphous  $\text{MoO}_x$  samples held at the temperature indicated.

Three different behaviours could be detected: At  $T < -123$  °C, the probe atoms come to rest in highly defective areas and are characterized as high spin  $\text{Fe}^{2+}$  with very low binding to the lattice. At  $-123^\circ\text{C} < T < 327$  °C, the probe atoms are characterized as high spin  $\text{Fe}^{2+}$  in amorphous state. At  $T > 327^\circ\text{C}$ , the shift of lines and decreased splitting evidences that the sites get more covalent character and exhibit stronger binding to the lattice; this happens when the  $\text{MoO}_x$  recrystallizes. Similar results were obtained using  $^{119}\text{In}$  (not shown here).

These results demonstrate that  $\text{MoO}_x$  is well suited for implantation (defects anneal at relatively low temperatures), but much further work is needed to understand the nature of the sites were obtained on amorphous samples, and one would need to investigate the differences on crystalline samples.

Concluding, PAC and eMS are unique probing methods where every radioactive nucleus reveals its local interaction with the system under study, the whole at very low

concentrations below 0.01%. Our collaboration includes the expertise of both material and nuclear applied physicists using these techniques at ISOLDE-CERN, a laboratory that provides a multitude of elements and isotopes adequate to the use of the PAC and eMS techniques in optimum experimental conditions. The present working program proposes the study of impurity doping and the study of point defects and its electronic configuration in molybdenum oxide, everything investigated from an atomic point of view.

## Summary of requested shifts:

We estimate the total amount of ISOLDE beam time needed to accomplish the above-described tasks to be 9 shifts, distributed according to table I:

Table I: Beam time request for PAC and eMS studies

Perturbed Angular Correlations Studies								
Required isotope	Implanted beam	Probe element	Type of experiment	Approx. Intensity [at/ $\mu$ C]	Target / Ion source	Required atoms per sample	Comments	n° of shifts
$^{111m}\text{Cd}(48\text{m})$	$^{111m}\text{Cd}$	$^{111}\text{Cd}$	$\gamma$ - $\gamma$ , $e^-$ - $\gamma$ PAC (*)	$10^8$	Molten Sn; plasma	$2 \times 10^{10}$	$\gamma$ - $\gamma$ PAC (10K – 1200K) $e^-$ - $\gamma$ PAC (50K-823K)	4
$^{117}\text{Cd}(2.49\text{h})$	$^{117}\text{Ag}$	$^{117}\text{In}$	$\gamma$ - $\gamma$ PAC	$10^8$	UC <sub>x</sub> ; RILIS (Ag)	$5 \times 10^{10}$	$\gamma$ - $\gamma$ PAC (10K – 1200K)	1
$^{115}\text{Cd}(53.46\text{h})$	$^{115}\text{Ag}$	$^{115}\text{In}$	$\beta$ - $\gamma$ PAC (**)	$10^8$	UC <sub>x</sub> ; RILIS (Ag)	$1 \times 10^{11}$	$\beta$ - $\gamma$ PAC (RT=300K)	1
Mossbauer Studies								
Required isotope	Implanted beam	Probe element	Type of experiment	Approx. Intensity [at/ $\mu$ C]	Target / Ion source	Required atoms per sample	Comments	n° of shifts
$^{57}\text{Mn}$ (1.5m)	$^{57}\text{Mn}$	$^{57}\text{Fe}$	eMS	$2 \times 10^8$	UC <sub>x</sub> , RILIS (Mn)	$1 \times 10^{12}$	Measurement temperatures below 850 K	1
$^{119}\text{In}$ (2.1m)	$^{119}\text{In}$	$^{119}\text{Sn}$	eMS	$2 \times 10^8$	UC <sub>x</sub> , RILIS (In)	$1 \times 10^{12}$	Measurement temperatures below 750 K	1
$^{151}\text{Gd}(120\text{d})$	$^{151}\text{Dy}(17.9\text{m})$ → $^{151}\text{Tb}(17.6\text{h})$ → $^{151}\text{Gd}(120\text{d})$	$^{151}\text{Eu}$	eMS	$1 \times 10^8$	Ta foil RILIS (Dy)	$2 \times 10^{12}$	Measurement temperatures below 750 K	0.5
$^{166}\text{Ho}(26.9\text{h})$	$^{166}\text{Ho}$	$^{166}\text{Er}$	eMS	$1 \times 10^9$	Ta foil, RILIS (Ho)	$2 \times 10^{10}$	Measurements done at 4K (LHe)	0.5

(\*) By comparing  $\gamma$ - $\gamma$  PAC with  $e^-$ - $\gamma$  PAC on the same sample we can check for the existence of long – lived ( $ns - \mu s$ ) electronic excited states at the probe atom triggered by the emission of the c.e.. In that case, electron mobility of the host can be probed via the study of the electronic recombination rates of the probe atom, as a function of measuring temperature. If the probe electronic recombination after emission of the c.e. is too fast – then  $\gamma$ - $\gamma$  PAC and  $e^-$ - $\gamma$  PAC show the same observable EFG frequencies what will serve, as well, as a cross check for the electronic equilibrium of the Cd probe after electron capture decay of  $^{111}\text{In} \rightarrow ^{111}\text{Cd}$ .

(\*\*) beta – gamma PAC uses beta decay parity violation, regarding the principal quantification axis here given by the orientation of the EFG principal axis V<sub>zz</sub>. On  $\beta$ - $\gamma$  PAC a sinus – like PAC observable function is observed as a function of time between detection of the beta and the gamma. From the sign of the sinus we infer the sign of the V<sub>zz</sub> principal axis component an important feature upon characterizing the incorporation of the probe atom in the crystalline lattice. These experiments require single crystals, being therefore possible to perform on the lamellar crystalline samples.

(\*\*\*) standard PAC is not limited by temperature within 0.1 K – 1773 K. The presented temperature ranges are due to the current experimental limitations.



Most of the required beam time consists of collections to be measured off-line and can in this way be easily shared with other users. We stress the particular case of the  $^{111m}\text{Cd}$  beam time, where collections should run day and night with a period of about 4 hours between collections that usually last for 15-30 min. There are actually four PAC setups co-shared during beam times and the samples can be implanted on the same collective sample holder together with other users running the same beam time. All isotopes for off-line measurements are collected in the general-purpose implantation chambers at GLM at the ISOLDE hall, building 170, and transported in sealed boxes according a safety procedure to the new Solid State Laboratory in building 508-R-008. There, off-line PAC and eMS experiments are performed after annealing and as function of temperature for the set of samples with different stoichiometry and doping.

The PAC collections for  $^{111m}\text{Cd}$  can be done together with the collections of the IS481, IS487, IS515 and IS585 experiments.

The PAC collections for  $^{117}\text{Ag}(^{117}\text{In})$  and  $^{115}\text{Ag}(^{115}\text{In})$  can be done together with the collections of the IS481, IS487, and IS585 experiments.

On-line measurements are required for the eMS studies with  $^{119}\text{In}$  and  $^{57}\text{Mn}$  where at least 3 temperature series on samples of different stoichiometry and doping (each temperature series takes 2 hours) are expected to be done. On selected samples we will make angular dependent measurements (1 hour) and quenching (implantation at high temperatures, measurements at liquid nitrogen temperatures, 1 hour). The measurements here will be done in connection with the IS576 and IS578 experiments.

The eMS collections for  $^{151}\text{Eu}$  samples ( $^{151}\text{Dy}$  implantations) can be done together with the collections of the IS528 experiments.

The eMS collections for  $^{166}\text{Er}$  samples ( $^{166}\text{Ho}$  implantations) can be done together with collections of the I161 experiment.

Several furnace systems exist already at the ISOLDE SSP lab, building 508-R-004, for annealing treatments under vacuum or gas flow at atmospheric pressure.

## References

[SCH1996] G. Schatz and A. Weidinger, 1996 Nuclear Condensed Matter Physics: Nuclear Methods and Applications (Chichester ; New York: John Wiley).

[ABRA1953] A. A. Bragg and R. V. Pound. Physical Review 92 n.4 (1953) 943.

<http://dx.doi.org/10.1103/PhysRev.92.943>

[BAI2014] S. Bai, C. Chen, D. Zhang, R. Luo, D. Li, A. Chen, C.-C. Liu, Sensors and Actuators B 204, 754–762 (2014).

<http://dx.doi.org/10.1016/j.snb.2014.08.017>

[BAL2013] M. Baldoni, L. Craco, G. Seifert and S. Leoni, J. Mater. Chem. A 1, 1778 (2013).

<http://dx.doi.org/10.1039/C2TA00839D>

[COM2005] E. Comini, L. Yubao, Y. Brando and G. Sberveglieri, Chem. Phys. Lett. 407, 368 (2005).



<http://dx.doi.org/10.1016/j.cplett.2005.03.116>

[COR2016] Private communication by J.G. Correia; The proof of concept has been obtained in several systems studied, e.g.,  $^{111m}\text{Ta}:\text{GaN}$ ,  $^{111}\text{In}:\text{Al}_2\text{O}_3$  among others, being the subject of undergoing thesis and papers (to be published).

[GIR2011] C. Girotto, E. Voroshazi, D. Cheyns et al., ACS Appl. Mater. Interfaces 3, 3244 (2011).

DOI: <http://dx.doi.org/10.1021/am200729k>

[HAN2011] Han-Yi Chen, Huan-Chieh Su, Chia-Hsiang Chen et al. J. Mater. Chem. 21, 5745 (2011).

<http://dx.doi.org/10.1039/c0jm03815f>

[HU2015] X. Hu, W. Zhang, X. Liu, Y. Mei and Y. Huang, Chem. Soc. Rev. 44, 2376 (2015).

<http://dx.doi.org/10.1039/C4CS00350K>

[LAB2001] M. Labanowska, ChemPhysChem 2, 712 (2001).

DOI:[http://dx.doi.org/10.1002/1439-7641\(20011217\)2:12<712::AID-CPHC712>3.0.CO;2-H](http://dx.doi.org/10.1002/1439-7641(20011217)2:12<712::AID-CPHC712>3.0.CO;2-H)

[LUP1996] D. Lupascu, S. Habenicht, K.-P. Lieb, M. Neubauer, M. Uhrmacher, and T. Wenzel, Phys. Rev. B54, 871 (1996)

<http://dx.doi.org/10.1103/PhysRevB.54.871>

[MAS2011] R. Más-Ballesté, C. Gómez-Navarro, J. Gómez-Herrero and F. Zamora, Nanoscale 3, 20 (2011).

<http://dx.doi.org/10.1039/C0NR00323A>

[MEY2012] J. Meyer, S. Hamwi, M. Kröger, W. Kowalsky, T. Riedl and A. Kahn, Adv. Mater. 24, 5408 (2012).

<http://dx.doi.org/10.1002/adma.201201630>

[PEN2014] Peng-Ru Huang, Yao He, Chao Cao and Zheng-Hong Lu, Sci. Rep. 4, 7131 (2014).

<http://dx.doi.org/10.1038/srep07131>

[SON2012] L.X. Song, J. Xia, Z. Dang, J. Yang, L.B. Wang and J. Chen CrystEngComm 14, 2675 (2012).

<http://dx.doi.org/10.1039/c2ce06567c>

[WAN2012] H.-Q. Wang, T. Stubhan, A. Osvet, et al., Solar Energy Materials & Solar Cells 105, 196 (2012).

<http://dx.doi.org/10.1016/j.solmat.2012.06.005>

[YAO1992] J. N Yao, K. Hashimoto and A. Fujishima, Nature 355, 6361 (1992).

<http://dx.doi.org/10.1038/355624a0>

[ZHO2003] J. Zhou, N.S. Xu, S.Z. Deng, J. Chen, J.C. She and Z.L. Wang, Adv. Mater. 15, 1835 (2003).

<http://dx.doi.org/10.1002/adma.200305528>

# Appendix

## 1 DESCRIPTION OF THE PROPOSED EXPERIMENT

The experimental setup comprises: *(name the fixed-ISOLDE installations, as well as flexible elements of the experiment)*

Part of the Choose an item.	Availability	Design and manufacturing
SSP-GLM chamber	<input checked="" type="checkbox"/> Existing	<input checked="" type="checkbox"/> To be used without any modification
Existing equipment on the solid state labs in building 508-r-002, r-004 and r-008	<input checked="" type="checkbox"/> Existing	<input checked="" type="checkbox"/> To be used without any modification <input type="checkbox"/> To be modified
- 6 detector PAC standard setups - annealing furnaces - glove boxes	<input type="checkbox"/> New	<input type="checkbox"/> Standard equipment supplied by a manufacturer <input type="checkbox"/> CERN/collaboration responsible for the design and/or manufacturing

## 2 Hazards generated by the experiment

*(if using fixed installation)* Hazards named in the document relevant for the fixed SSP-GLM chamber and building 508-r-002, r-004 and r-008 installations. Every experiment has its one written procedure file discussed with Radio Protection services, before every beam time.

Additional hazards:

Hazards			
	SSP-GLM	Building 508	[Part 3 of the experiment/equipment]
Thermodynamic and fluidic			
Pressure	Vacuum [Bar], 10[l]	Ambient	
Vacuum	10-6 mbar at SSP chamber 10 during collections	none	
Temperature	77K due to implantations on ice.	Ambient 20 – 15°C	
Heat transfer			
Thermal properties of materials	-		
Cryogenic fluid	Liquid nitrogen. Ice is kept at a cold finger adapted to a metallic LN2 15 litres Dewar. The system is of current use since 2001, being set at the	Liquid nitrogen, 1 Bar, few litres used during the PAC measurements on appropriate Dewar.	

	back of the SSP Chamber.		
<b>Electrical and electromagnetic</b>			
Electricity	[voltage] [V], [current][A]		
Static electricity			
Magnetic field	[magnetic field] [T]		
Batteries	<input type="checkbox"/>		
Capacitors	<input type="checkbox"/>		
<b>Ionizing radiation</b>			
Target material	[material]		
Beam particle type (e, p, ions, etc)			
Beam intensity			
Beam energy			
Cooling liquids	[liquid]		
Gases	[gas]		
Calibration sources:	<input type="checkbox"/>		
• Open source	<input checked="" type="checkbox"/> Produced at ISOLDE:	<input checked="" type="checkbox"/> Produced at ISOLDE:	
• Isotope	111mCd(48m) 117Cd(2.49h) 115Cd(53.46h) 57Mn (1.5m) 119In (2.1m) 151Gd(120d) 166Ho(26.9h)	111mCd(48m) 117Cd(2.49h) 115Cd(53.46h) 151Gd(120d) 166Ho(26.9h)	
• Activity (per sample and measurement)	111mCd(48m) < 5.50E+06 Bq 117Cd(2.49h) < 3.87E+06 Bq 115Cd(53.46h) < 3.60E+05 Bq 57Mn (1.5m) < 5E+08 Bq (online in saturation) 119In (2.1m) < 1E+09 Bq (online in saturation) 151Gd(120d) < 1.34E+05 Bq 166Ho(26.9h) < 1.43E+05 Bq	111mCd(48m) < 5.50E+06 Bq 117Cd(2.49h) < 3.87E+06 Bq 115Cd(53.46h) < 3.60E+05 Bq 151Gd(120d) < 1.34E+05 Bq 166Ho(26.9h) < 1.43E+05 Bq	
• Dose rate on contact and in 10 cm distance (per sample and measurement)	[dose][mSV] 111mCd(48m) ~ 0.5 mSv/h 117Cd(2.49h) ~ 0.5 mSv/h 115Cd(53.46h) ~ 32 μSv/h 57Mn (1.5m) ~ 75 mSv/h (online in saturation) 119In (2.1m) ~ 75 mSv/h (online in saturation) 151Gd(120d) ~ 12 μSv/h 166Ho(26.9h) ~ 13 μSv/h	[dose][mSV] 111mCd(48m) ~ 0.5 mSv/h 117Cd(2.49h) ~ 0.5 mSv/h 115Cd(53.46h) ~ 32 μSv/h 151Gd(120d) ~ 12 μSv/h 166Ho(26.9h) ~ 13 μSv/h	[dose][mSV]
Use of activated material:	None	none	none
• Description	<input type="checkbox"/>	<input type="checkbox"/>	<input type="checkbox"/>
• Dose rate on contact and in 10 cm distance	[dose][mSV]	[dose][mSV]	[dose][mSV]
• Isotope			
• Activity			
• Sealed source	<input checked="" type="checkbox"/> [ISO standard]	<input checked="" type="checkbox"/> [ISO standard]	
• Isotope	22Na sources provided by RP services at CERN	22Na sources provided by RP services at CERN	
• Activity	< 3e7 Bq	< 3e7 Bq	
<b>Non-ionizing radiation</b>			
Laser	none		
UV light	none		

Microwaves (300MHz-30 GHz)	none		
Radiofrequency (1-300MHz)	none		
<b>Chemical</b>			
Toxic	Mo-oxides: potentially toxic	Mo-oxides: potentially toxic	
Harmful	Acetone (ICSC: 0087), Ethanol (ICSC: 0044) Methanol (ICSC: 0057). Less than few centilitres per chemical, used on cleaning samples on ventilated fume hood on building 508-r-002.  <i>The respective ICSC forms have been printed and are handled during preparation and experiments.</i>	Acetone (ICSC: 0087), Ethanol (ICSC: 0044)	
CMR (carcinogens, mutagens and substances toxic to reproduction)	[chemical agent], [quantity]		
Corrosive	[chemical agent], [quantity]		
Irritant	[chemical agent], [quantity]		
Flammable	[chemical agent], [quantity]		
Oxidizing	[chemical agent], [quantity]		
Explosiveness	[chemical agent], [quantity]		
Asphyxiant	[chemical agent], [quantity]		
Dangerous for the environment			
<b>Mechanical</b>			
Physical impact or mechanical energy (moving parts)	[none]		
Mechanical properties (Sharp, rough, slippery)	[none]		
Vibration	[none]		
Vehicles and Means of Transport	[none]		
<b>Noise</b>			
Frequency	[frequency],[Hz] Ambient noise at the ISOLDE Hall, building 170		
Intensity			
<b>Physical</b>			
Confined spaces	[none]		
High workplaces	[none]		
Access to high workplaces	[none]		
Obstructions in passageways	[none]		
Manual handling	All samples and sample holders are manually handled either by long tweezers to insert and extract the sample holder into and out of the SSP implantation chamber at GLM, or when manipulating	All samples and sample holders are manually handled either by long tweezers to insert and extract the sample holder into and out of the SSP implantation chamber at GLM, or when manipulating	

	<p>the samples and sample holders inside glove boxes or fume hoods on building 508-r-002, r004 and r-008.</p> <p>On-line measurements on 57Mn and 119In are done at GLM with users outside the brick shielded setup</p>	<p>the samples and sample holders inside glove boxes or fume hoods on building 508-r-002, r004 and r-008.</p>	
Poor ergonomics	[none]		

## 2.1 Hazard identification

### **Classification according to Regulation (EC) No 1272/2008 [EU-GHS/CLP]**

Carcinogenicity (Category 2)

Eye irritation (Category 2)

Specific target organ toxicity - single exposure (Category 3)

### **Classification according to EU Directives 67/548/EEC or 1999/45/EC**

Limited evidence of a carcinogenic effect. Irritating to eyes and respiratory system.

There will be a specific protocol to be followed before every beam time. Example: edms number 1569671 v.1.

## 3.2 Average electrical power requirements (excluding fixed ISOLDE-installation mentioned above): (make a rough estimate of the total power consumption of the additional equipment used in the experiment)

There is no additional equipment with relevant power consumption on these small-scale experiments.